Thermal Performance and Integration of Digital Systems in a Water-to-Water Thermoelectric Heat Pump

Oleg Ivanov
Poltava State Agrarian University, Skovorody Str. 1/3, 36001 Poltava, Ukraine
oleegivanov@yahoo.com

Keywords: Thermoelectric Converter, Peltier Effect, Energy Conversion Efficiency, Thermal Power, Electric Current, Heat Pump.

Abstract: This Paper Investigates the thermal performance of a water-to-water thermoelectric heat pump through the integration of a custom digital monitoring and control system. The study aimed to utilize this system for the experimental determination of the coefficient of performance (COP) under variable influencing factors. Heat transfer was carried out due to the Peltier effect, where the flow of electric current through the converter simultaneously caused heat absorption and heat emission at its thermal sides. Heat exchange on each side was implemented by forced circulation of liquid heat carriers. At one stage of the experiment, the variation of temperature indicators on each side of the converter was investigated with increasing electric current in the range of 3–9 A. On the hot side, the temperature increased linearly from 23.6 °C to 39 °C, while on the cold side it decreased nonlinearly from –4.8 °C to –18.56 °C. At another stage, under steady heat exchange conditions with varying current and heat carrier temperatures, the absorbed and emitted heat and the electrical power consumption of the system were determined. With increasing current, the heat emission Qhot rose linearly from 22 to 118 W, while the electrical power consumption of the heat pump varied quadratically from 16.9 to 155.65 W. The maximum COP reached 135.5%, but decreased exponentially with increasing current, crossing the economically viable threshold of 100% at 7 A. The best results were obtained when transforming thermal energy from a low-temperature source at 15 °C to a high-temperature source at 20 °C.

1 INTRODUCTION

Until recently, thermal energy for heating residential, industrial, commercial, and other spaces was predominantly generated using heat sources based on the combustion of hydrocarbon fuels extracted from the Earth. However, the rising cost of these fuels has raised concerns regarding their long-term viability as primary energy sources [1].

A range of alternative approaches and thermotechnical devices has emerged, offering improved operational performance and cost-effectiveness [2]. These include heat generators utilizing various types of solid biomass, such as wood, compressed hay and straw, and other plant residues capable of producing substantial thermal energy upon combustion [3].

Heat pumps represent another promising alternative [4]. They generate thermal energy by performing a refrigeration cycle that absorbs dispersed heat from the surrounding environment. Sources of this heat include geothermal reservoirs (soil layers, surface and underground waters) and ambient air masses [5], [6].

Conventional heat pumps typically employ freon-based refrigeration machines containing low-boiling working fluids with high cooling capacity [7], [8]. Their use may pose risks of toxicity, equipment damage, and operational accidents [9]. Moreover, such systems are often bulky and require specialized expertise for operation and maintenance [10].

Therefore, there is a growing need for heat pumps that retain the advantages of this technology while avoiding its drawbacks. Thermoelectric heat pumps based on the Peltier effect represent one potential solution, enabling heat transfer from low- to high-temperature sources through the consumption of electrical energy. Unlike conventional thermoelectric generators [11], where heat flux induces an electric potential difference at the contacts, thermoelectric heat pumps incorporate compact, lightweight, and operationally reliable energy converters [12]. However, their relatively low conversion efficiency and high cost remain limiting factors, which

motivates ongoing research aimed at improving performance and reducing operational expenses.

2 MATERIALS AND METHODS

2.1 Laboratory Setup

The aim of this study is to determine the coefficient of performance (COP, η) of a water-to-water thermoelectric heat pump. The schematic diagram of the heat pump is shown in Figure 1.

The main component of the system is a thermoelectric converter operating based on the Peltier effect. This converter has two opposing thermal sides: the "hot" side, where heat is released, and the "cold" side, where heat is absorbed. A direct current (DC) power source is required to transfer thermal energy from one side of the converter to the other. In this study, a laboratory power supply with adjustable output parameters was used as the DC source.

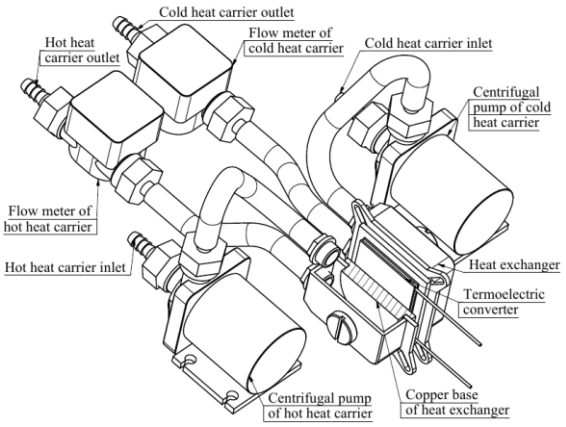

Figure 1: Schematic diagram of a water-to-water thermoelectric heat pump.

To ensure heat exchange between the heat carriers and the thermal sides of the thermoelectric converter, heat exchangers with heat-conducting elements in contact with the converter are used. Thermally conductive paste is applied between the contact surfaces to improve thermal contact and reduce thermal resistance.

Circulation of the liquid heat carriers through the heat exchangers is provided by two separate centrifugal pumps. The flow rates of these pumps are regulated via PWM controllers to ensure stable and controlled circulation.

Distilled water is used as the working fluid responsible for heat and mass transfer in the heat pump. Two separate liquid streams at different temperatures are maintained to simulate the operational conditions of the system. Thermal conditioning of both heat carriers is carried out in individual calorimetric tanks.

In one tank, the thermal state of the heat carrier, from which heat is extracted by the heat pump, is restored using a resistive heater. The temperature of the heat carrier in this tank is controlled by an electronic thermostat. Restoration of the thermal state of the heat carriers is necessary to maintain a stable temperature regime for the operation of the heat pump with a closed hydraulic circuit.

The overall view of the laboratory prototype of the heat pump, including all necessary control and measurement equipment, is shown in Figure 2.

Figure 2: Experimental setup for investigating the operation of the heat pump.

This laboratory configuration provides the physical foundation required for controlled thermal and hydraulic experimentation. However, to ensure accurate tracking of all operational parameters and to maintain stable experimental conditions, the system must be complemented by a dedicated digital monitoring and control architecture.

2.2 Architecture of the Digital Monitoring System

This subsection presents the instrumentation responsible for monitoring, measuring, and recording all key thermal and electrical parameters of the experimental setup.

Digital temperature sensors (DS18B20) are employed to monitor the temperature changes of the heat carriers before and after heat exchange in the heat exchangers. These sensors are installed in the supply pipelines near the heat exchanger inlets and outlets.

The flow rate of the heat carriers is measured using a contact method in volumetric units. Volumetric flow meters YF-S401 and SEN-HZ21WA, with different measurement ranges, are used to accommodate varying operating conditions.

The temperatures of the heat-exchange surfaces of the thermoelectric converter are measured using resistive temperature sensors, which are mounted directly on the contact surfaces.

The electrical parameters of the thermoelectric converter are measured using digital voltmeters and ammeters, providing complete monitoring of its operating characteristics.

A digital monitoring system based on an 8-bit Atmega328 microcontroller was developed to process signals from both analog and digital sensors. This system performs real-time tracking of the control parameters over time, records the data in the memory of a removable storage device, displays the measurements on an information panel, and transmits them wirelessly to the researcher's personal digital device for further analysis.

PWM controllers used for pump regulation, DS18B20 temperature sensors, the Atmega328-based monitoring unit, and the wireless transmission module constitute the complete digital monitoring and control subsystem integrated into the experimental setup.

2.3 Experimental Procedure

This subsection describes the sequence of actions taken to perform the experimental investigation and obtain the data required for calculating COP.

In accordance with the study aim, a set of experimental research tasks was formulated.

The first task is to determine the maximum temperatures on the thermal sides of the thermoelectric converter at different values of electric current. Based on the technical documentation of the thermoelectric converter, a range of current values was established. This range spans 6 A, with current values varying from 3 to 9 A in increments of 1 A.

The thermoelectric converter is connected to a power supply with a current limit set within the selected range. Subsequently, the heat carrier is supplied to the heat exchanger installed on the heat-releasing side of the converter at a constant temperature of approximately 20 °C and a predetermined flow rate. Adjusting the flow rate allows for the regulation and maintenance of a stable heat absorption process on the heat-releasing side. No heat carrier is supplied to the heat exchanger on the heat-absorbing side, thus excluding any external heat input.

The passage of electric current through the thermoelectric elements of the converter induces a temperature difference between its thermal sides. Over time, this temperature difference gradually increases, and when it reaches its maximum value, the temperature extrema are recorded.

After the completion of each experiment, a time interval is allowed for all components of the heat pump to equalize their temperatures to 20 °C. Once thermal equilibrium is restored, similar experiments are conducted at different current values within the specified range.

The second task is to determine the amount of thermal energy released and absorbed on the thermal sides of the thermoelectric converter when varying the electrical power consumption under steady-state heat exchange conditions. The coefficient of performance (COP) of the heat pump is calculated as the ratio of the heat output on the hot side to the electrical power input.

Implementation of this task involves conducting a two-factor experiment, the methodology of which is outlined as follows. After connecting the thermoelectric converter to the power supply, the required current value is set according to the ammeter within the range of 3 to 9 A. Simultaneously, the circulation pumps supply the heat carriers to the recuperative heat exchangers. One heat carrier (hot) functions as the absorber of thermal energy and is directed to the heat exchanger on the heat-releasing side of the converter. The other heat carrier (cold) serves as the heat source, from which thermal energy is extracted on the heat-absorbing side via the corresponding heat exchanger.

Throughout the entire series of experiments, the hot heat carrier is maintained at a constant temperature of 20 °C. In contrast, the temperature of the cold heat carrier varies depending on the specific experimental series, taking values from a set range of 10, 15, or 20 °C. Supplying the cold heat carrier to the heat exchanger at the desired temperature, as defined by the experimental sequence and conditions, is achieved through prior thermal conditioning in a calorimetric tank from which the fluid is drawn immediately before each test.

The duration of each experiment is 8 minutes, starting from the moment a steady-state heat exchange regime is achieved on each of the heat exchanger sides.

Each experiment is repeated several times at different current values with a fixed increment, while maintaining the previously set temperature of the cold

heat carrier constant to ensure statistical reliability of the results.

3 RESULTS AND DISCUSSIONS

Figure 3 illustrates the trends in temperature variations on the thermal sides of the thermoelectric converter, as well as the temperature difference between these sides, depending on the magnitude of the electric current passing through the converter's electrical circuit.

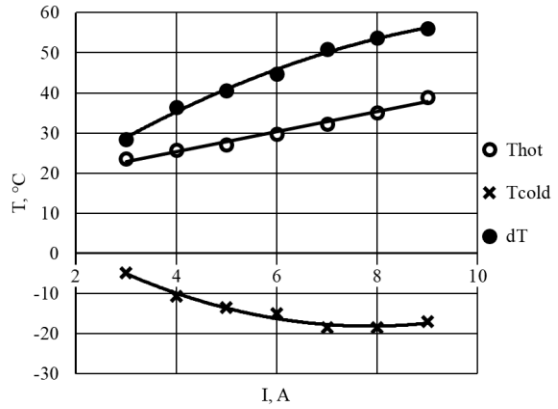

Figure 3: Dependence of the main thermotechnical parameters of the heat pump on the electric current magnitude.

According to the presented data, the temperature on the hot side (Thot) exhibits a general trend of linear increase throughout the entire range of current variation. On average, the temperature rises by approximately 2.5°C for every 1 A increase in current. At the boundary points of this dependency, the temperature reaches 23.6°C at 3 A and 39°C at 9 A.

The temperature behavior on the cold side (Tcold) differs notably from that of the hot side. Specifically, Tcold changes in a nonlinear manner and exhibits an inflection point at a certain current value. As the current increases from 3 A to 8 A, Tcold continuously decreases from –4.8 °C to –18.56 °C. Beyond 8 A, this trend reverses, and the temperature rises to –17.06 °C. This reversal is caused by the increasing thermal backflow between the sides, which induces heat transfer through thermal conductivity from the hot side to the cold side, partially slowing down and offsetting the further decrease of Tcold. Nevertheless, despite the differences in behavior between Tcold and Thot, the temperature difference continues to grow steadily, reaching a maximum of 56.06 °C at 9 A.

In addition to influencing the temperature profiles of the thermal sides, the current value also affects other thermotechnical parameters. As shown in Figure 4, the electric current determines the variations in the amount of thermal energy absorbed on the cold side (Qcold), the heat released on the hot side (Qhot), and the coefficient of performance (COP, η), which characterizes the thermal energy conversion of the heat pump.

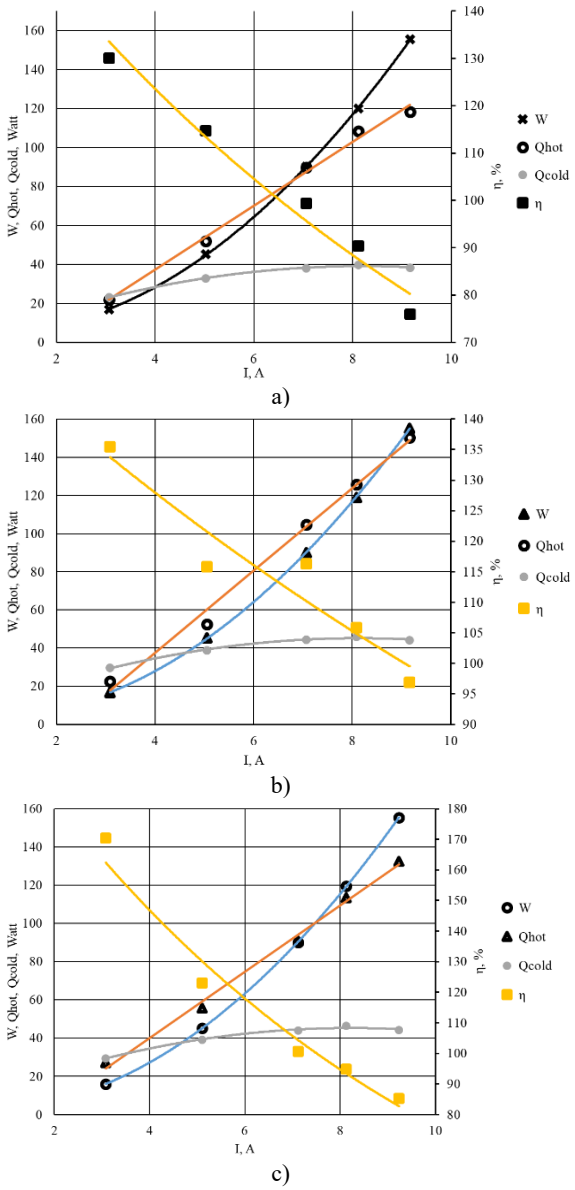

Figure 4: Dependence of the main thermotechnical parameters of the heat pump on the electric current magnitude, where a) Thot=20°C, Tcold=10°C; b) Thot=20°C, Tcold=15°C; c) при Thot=20°C, Tcold=20°C.

The experimental results presented in Figure 4a, obtained under heat extraction from the cold heat carrier at 10°C, demonstrate an almost linear increase over time in the amount of heat Qhot generated on the hot side of the thermoelectric converter and removed by the hot heat carrier.

The regression-based approximation for Qhot as a function of electric current is as follows:

$$Q_{hot} = 16.409 \cdot I - 28.395 \quad (1)$$

The intensity of thermal energy extraction by the heat carrier averages 16 W per unit of electric current, with the thermal flow varying between 22 and 118 W.

In contrast, the heat absorption Qcold follows a nonlinear trend, exhibiting both increasing and decreasing segments. As the current varies from 3 A to 8 A, the heat absorbed from the cold heat carrier increases, reaching 36.7 W. With a further increase to 9 A, Qcold decreases slightly by 1.5 W, stabilizing at 38.3 W. The regression-based approximation for the relationship between absorbed heat and electric current is as follows:

$$Q_{cold} = -0.6076 \cdot I^2 + 9.967 \cdot I - 1.7511. \quad (2)$$

The electrical power of the heat pump, W, is described by a quadratic function and increases from 16.9 W to 155.65 W. The regression-based approximation for the electrical power variation is given by:

$$W = 2.0664 \cdot I^2 - 2.6233 \cdot I + 5.7417. \quad (3)$$

The variation of the coefficient of performance (η) under the given conditions can be represented by an exponential curve, gradually decreasing with increasing electric current, ranging from 130.1% to 76%. The heat pump operates with a coefficient of performance above 100% - the threshold for COP > 1 operation - up to a current of 7 A. Beyond this point, further increases in current do not lead to the generation of Qhot exceeding the required electrical input.

Increasing the temperature of the cold heat carrier to 15°C positively affects the heat pump's performance across all comparative parameters (Fig. 4b). In particular, the amount of heat Qhot generated on the hot side per unit of time increases significantly, ranging from 22.5 to 150.4 W.

The regression-based linear approximation for Qhot is given by:

$$Q_{hot} = 21.552 \cdot I - 48.675. \quad (4)$$

The increase in Qhot is associated with enhanced heat absorption on the cold side of the converter. In the current range from 3 A to 9 A, Qcold varies from 29.6 to 44.2 W, reaching a maximum of 45.8 W at 8 A. This behavior can be represented by a quadratic function:

$$Q_{cold} = -0.6202 \cdot I^2 + 10.087 \cdot I + 4.1711. \quad (5)$$

The improvement of heat exchange processes on both sides of the thermoelectric converter, while maintaining a constant electrical energy consumption, is reflected in the enhanced thermal energy conversion efficiency, with the coefficient of performance η remaining above 100% throughout the entire current range. Under these conditions, the coefficient of performance η varies between 100% and 135.5%.

Experimental investigations at a cold heat carrier temperature of 20°C (Fig. 4c) reveal results opposite to those observed previously, regarding heat transfer on the thermal sides of the converter. The first notable difference is a slight reduction in heat generation, reflected in a decrease in thermal energy delivered to the hot heat carrier, as illustrated in Figure 5.

With a cold heat carrier at 20°C, heat production by the heat pump decreases on average by 10–13% compared to operation with a cold heat carrier at 15°C. Conversely, using a cold heat carrier at 10°C results in a 10–12% increase in the heat delivered to the hot heat carrier.

Meanwhile, the amount of heat extracted from the cold heat carrier remains nearly constant, following a parabolic trend within 29.4–46.3 W. Initially, Qcold increases with rising current, reaching 46.3 W at 8 A, and then gradually decreases to 44.2 W after reaching this maximum.

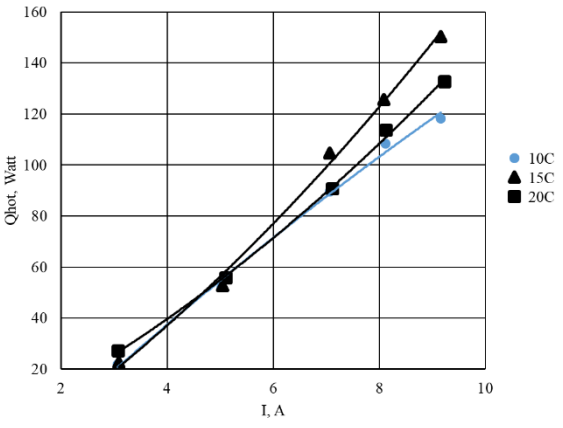

Figure 5: Heat generation capacity of the thermoelectric heat pump at different cold heat carrier temperatures.

The deterioration in heat production quantitatively affects the reduction of the thermal energy conversion performance, particularly in the 7 - 9 A current range, where the coefficient of performance η drops below 100%, reaching a minimum value of 85.3%.

4 CONCLUSIONS

The analysis of the thermoelectric heat pump's performance, based on experimental investigations, demonstrated a relatively high level of thermal energy conversion performance. The coefficient of performance (η) of the heat pump, over a wide range of electrical energy input, varies between 100% and 130.1% (COP = 1.0–1.301).

The successful integration of the digital monitoring and control system was crucial for obtaining high-precision, real-time data on key thermotechnical parameters, ensuring the reliability of the experimental results. The developed system also demonstrates a scalable approach for data acquisition and process control in laboratory and applied thermal energy systems.

This type of heat pump can be effectively applied for heating localized workspaces, residential areas, or small-volume rooms, provided that a readily available source of free heat and inexpensive electrical energy are accessible.

To generate a substantial amount of thermal energy using this heat pump, a significant increase in the number of thermoelectric converters would be required, while ensuring favorable conditions for both heat emission and heat absorption.

REFERENCES

[1] A. Komorowska and T. Surma, "Comparative analysis of district heating markets: examining recent prices, regulatory frameworks, and pricing control mechanisms in Poland and selected neighbouring countries," Polityka Energetyczna – Energy Policy Journal, vol. 27, no. 1, pp. 95–118, 2024, doi: 10.33223/epj/175328.

[2] P. Lorenzen and C. Alvarez-Bel, "Variable cost evaluation of heating plants in district heating systems considering the temperature impact," Applied Energy, vol. 305, p. 117909, 2022, doi: 10.1016/j.apenergy.2021.117909.

[3] V. Stanytsina, V. Artemchuk, O. Bogoslavska, I. Zinovieva, and N. Ridei, "The influence of environmental tax rates on the Levelized cost of heat on the example of organic and biofuels boilers in Ukraine," E3S Web of Conferences, vol. 280, p. 09012, 2021, doi: 10.1051/e3sconf/202128009012.

[4] A. Toleikyte et al., The Heat Pump Wave: Opportunities and Challenges, Luxembourg: Publications Office of the European Union, 2023, doi: 10.2760/27877.

[5] P. P. Altermatt, J. Clausen, H. Brendel et al., "Replacing gas boilers with heat pumps is the fastest way to cut German gas consumption," Communications Earth & Environment, vol. 4, p. 56, 2023, doi: 10.1038/s43247-023-00715-7.

[6] M. J. S. Zuberi, J. Chambers, and M. K. Patel, "Techno-economic comparison of technology options for deep decarbonization and electrification of residential heating," Energy Efficiency, vol. 14, p. 75, 2021, doi: 10.1007/s12053-021-09984-7.

[7] A. Zini, L. Socci, G. Vaccaro, A. Rocchetti, and L. Talluri, "Working fluid selection for high-temperature heat pumps: A comprehensive evaluation," Energies, vol. 17, no. 7, p. 1556, 2024, doi: 10.3390/en17071556.

[8] J. Nie, K. Wang, X. Kong, H. Zhang, and S. Zhang, "Theoretical study and experimental validation on the applicable refrigerant for space heating air source heat pump," Sustainability, vol. 15, no. 12, p. 9420, 2023, doi: 10.3390/su15129420.

[9] A. K. Vuppaladadiyam, E. Antunes, S. S. V. Vuppaladadiyam, Z. T. Baig, A. Subiantoro, G. Lei, S.-Y. Leu, A. K. Sarmah, and H. Duan, "Progress in the development and use of refrigerants and unintended environmental consequences," Science of The Total Environment, vol. 823, p. 153670, 2022, doi: 10.1016/j.scitotenv.2022.153670.

[10] J. J. Aguilera, W. Meesenburg, T. Ommen, W. B. Markussen, J. L. Poulsen, B. Zühlsdorf, and B. Elmegaard, "A review of common faults in large-scale heat pumps," Renewable and Sustainable Energy Reviews, vol. 168, p. 112826, 2022, doi: 10.1016/j.rser.2022.112826.

[11] O. Ivanov, Study of the Energy Efficiency of a Thermal Electrical Generator with a Hydraulic Heat Supply System, Universitäts- und Landesbibliothek Sachsen-Anhalt, 2024, doi: 10.25673/118129.

[12] U. Tomc, S. Nosan, B. Vidrih, S. Bogić, K. Navickaite, K. Vozel, M. Bobič, and A. Kitanovski, "Small demonstrator of a thermoelectric heat-pump booster for an ultra-low-temperature district-heating substation," Applied Energy, vol. 361, p. 122899, 2024, doi: 10.1016/j.apenergy.2024.122899.